FINITE ELEMENT DESIGN OF BEARINGLESS PERMANENT MAGNET MOTORS

Wolfgang Amrhein, Siegfried Silber, Klaus Nenninger
Johannes Kepler University
Department of Power Electronics and Electrical Drives
Altenberger Straße 69
A-4040 Linz, Austria

SUMMARY

In high performance applications with high demands on speed range, lifetime, cleanness or tightness, magnetic bearing systems can provide substantial advantages to classical drive systems using ball or sliding bearings. Some of these applications like pumps, blowers or fans require only three actively controlled degrees of freedom and can be supported by four coil bearingless permanent magnet motors. In these cases three degrees of freedom are passively stabilized by the tensible force of permanent magnets.

Depending on the particular application an interior or exterior rotor design of the bearingless motor may be advantageous. A finite element analysis is used to show the interactions between the current density distributions of the stator and the excitation fields of the rotor. Different permanent magnet magnetization forms are examined. It is shown that the results of the interior rotor design differ significantly from the results achieved by exterior rotor design.

INTRODUCTION

In high performance applications with high demands on speed range, lifetime, cleanness or tightness, classical drive systems using ball or sliding bearings can get technical problems. Typical applications are spinning drives, high speed cutting milling machines, turbo compressors, blowers for mainframes, or pumps for the medical or chemical industry. In most of these high technology applications magnetic bearing systems are already used. Depending on the required number of actively controlled degrees of freedom magnetic bearing systems can be equipped with separate devices like radial bearings, axial bearings and motors or as in the case of only three actively controlled degrees of freedom with merely one bearingless drive.

In the last ten years a lot of research work has been done to work out different conceptions for bearingless drives, i.e. drives with integrated winding systems for generating torque as well as radial forces. There are several proposals based on the principle of induction machines, reluctance machines and synchronous permanent magnet motors [3]-[11].

In applications with only three actively controlled degrees of freedom and especially in pump applications, where the non-ferromagnetic pump housing is placed inside the motor air gap, a significant magnetization is necessary to establish the air gap field. In these cases, it is more efficient to use permanent magnet motors instead of electrically excited induction or reluctance motors. Figure 1 shows two examples of a bearingless pump design with an interior and exterior permanent magnet rotor.

In [1], [2] new bearingless permanent magnet motor types were presented by the authors. These motors use only four coils to generate both the radial levitation forces and the torque. In contrast to former proposals with considerably higher numbers of coils, there are some significant differences concerning the design and the functional principle. Table 1 shows a comparison of the two concepts with their substantial differences.

Table 1. Comparison of Bearingless Motors: Classical and Single-Phase Design

	classical bearingless motor	**single-phase bearingless motor**
winding concept	one winding (radial force control) one winding (torque control)	only one winding
number of phases	three phases (radial force control) three phases (torque control)	four phases (radial force and torque control)
armature fields	rotatory field (radial force control) rotatory field (torque control)	rotatory field (radial force control) alternating field (torque control)
field harmonics	suppressed by chorded and distributed windings	concentrated windings
armature currents	separate currents for radial force and torque control	current components superposed in the current controller
number of coils	depending on the motor design, but much higher than four (typically about 20)	four coils
radial force vector locus curve	radial force amplitude independent from the rotor angle (circular shape)	amplitude depends on the rotor angle (non-circular shape)

Figure 2 presents the constructional principle of the built and tested prototype in exterior rotor design [2], which is characterized by the features mentioned in the last row of table 1.
For the design of the bearingless motor it is very useful to get information about the specific force and torque characteristic using analytical [1,2] or finite element calculation methods. Depending on the application an interior or exterior rotor design can be more advantageous. The following part of the paper will show main differences between these two construction variants. The analysis has been done under the support of the finite element calculation program FEMAG.

FIELD AND FORCE COMPUTATIONS

For time-invariant field problems the system of Maxwell equations can be described by two electrostatic and two magnetostatic equations. The magnetostatic part is defined by the following set of equations

$$\nabla \times \mathbf{H} = \mathbf{J} \tag{1}$$
$$\nabla \cdot \mathbf{B} = 0 \tag{2}$$

where **H** defines the magnetic field intensity, **J** the electric current density and **B** the magnetic flux density.
Further the interaction between **B** and **H** has to be defined by a material specific equation

$$\mathbf{B} = \mu \mathbf{H} + \mathbf{M} \tag{3}$$

where **M** denotes the magnetization of the material.
Since $\nabla \cdot \mathbf{B} = 0$, **B** can be represented as a curl of the vector potential $\mathbf{A_p}$

$$\nabla \times \mathbf{A_p} = \mathbf{B}, \tag{4}$$

i. e. if vector potential $\mathbf{A_p}$ is known the flux density **B** can be calculated using (4).
The vector potential is solved numerically by

$$\nabla \times \frac{1}{\mu} \nabla \times \mathbf{A_p} = \nabla \times \mathbf{H} = \mathbf{J}. \tag{5}$$

The numerical computation of the forces acting on the rotor or the stator of the bearingless motor uses Maxwell's force tensor.

Using Maxwell's force tensor, it is supposed that the magnetic field intensity **H** is known on the surface enclosing the body. It's also supposed that this body is located in air with $\mu = \mu_0$.
With a differential area ds on the surface and an unit vector **n** normal to the surface (with **ds**=**n**ds) Maxwell's tensor is defined by the general expression

$$\mathbf{dF} = -\frac{\mu_0}{2} H^2 \mathbf{ds} + \mu_0 (\mathbf{H} \cdot \mathbf{ds}) \mathbf{H}. \tag{6}$$

or as magnetic pressure

$$\frac{\mathbf{dF}}{\mathrm{ds}} = -\frac{\mu_0}{2} H^2 \mathbf{n} + \mu_0 (\mathbf{H} \cdot \mathbf{n}) \mathbf{H} \tag{7}$$

The total force acting on the body is given by the integration of the magnetic pressure over the whole surface.

SIMPLIFICATION OF THE MOTOR MODEL

The magnetic circuit of the motor shown in figure 2 can be simplified by the use of a slotless motor design with an infinite thin current layer at the stator surface in the air gap. The magnetomotive force distribution of the air gap winding should have equivalent values as in the slotted design. The proposed simplification usually shows a good correspondence between calculations and measurements concerning radial forces and the mean value of the torque. Angle dependent torque variations due to the slotting of the stator don't occur in the motor model and therefore have to be neglected.

The forces acting on the rotor or the stator model can be divided into two parts: the Lorentz force components acting on the current layer and the Maxwell components acting on the ferromagnetic material.

For two-dimensional field problems with the condition for the ferromagnetic permeability $\mu_{fe} >> \mu_0$ the two components can be derived from (7) in the following way

$$\frac{dF(\varphi)}{ds} = \begin{pmatrix} \frac{B_n^2(\varphi)}{2\mu_0} \\ 0 \\ 0 \end{pmatrix} + \begin{pmatrix} -\frac{1}{2}\mu_0 A^2(\varphi) \\ A(\varphi)B_n(\varphi) \\ 0 \end{pmatrix}. \tag{8}$$

with B_n as normal component of the flux density B and A as the current density distribution along the stator surface. In (8) the first row of the vectors denotes the normal and the second row the tangential pressure components. Usually the normal component of the Lorentz vector can be neglected.

INTERIOR ROTOR DESIGN

Depending on the specifications of the application, the decision about the motor design either with interior or exterior rotor has to be made. As the following analyses will show there are differences not only in the mechanical design but also from the magnetic point of view.

Figure 3 presents an example of a motor model in interior rotor design. The stator comprises four concentrated coils. The rotor is equipped with four cylindrical permanent magnets which provide approximately a rectangular magnetic field distribution in the air gap. Depending on the phase currents a two pole armature field as well as a four pole armature field can be produced by the stator windings. According to the supposed motor design the two pole field is used for levitation force and the second field for torque control.

For the computation of the characteristic levitation force locus curve it is supposed that the rotor is turned while the phase currents are constant and the currents in two opposite slots compensate each other whereas the currents in the other two slots have the same amplitude and direction. In this case we get the two pole armature configuration.

Figure 4 shows the force vectors computed using (8) for different rotor angle steps. The force amplitudes in the two main axes of the diagram differ significantly. This effect is also demonstrated by figures 5 and 6 which show the flux density distribution of the motor in two orthogonal positions (rotor angle $\delta_1=0°$; $\delta_2=90°$). There are different reasons which are responsible for this behavior. One reason is the substantial influence of harmonics in the current and field distribution. The magnetic conditions are not comparable to idealized conditions with sinusoidal current and field distributions which would lead to a circular levitation force locus curve. Another reason are the different directions of rotation concerning the Lorentz and the Maxwell force vectors. Figure 7 and 8 illustrate the two force components separately.

A better performance can be achieved by a sinusoidal permanent magnet field distribution. The corresponding levitation force curve is presented in figure 9. In this case the force locus curve has an elliptical shape. With appropriate corrective currents in the motor windings the levitation forces can be produced in all directions. This would not be possible using the motor design with rectangular magnetic field distribution shown in figure 3.

EXTERIOR ROTOR DESIGN

The corresponding motor model design of figure 3 is shown in figure 10. The only difference is that in this motor design the rotor is outside the stator. The dimensions of the air gap diameter and the magnet height as well as the current distribution are the same. In contrast to the interior rotor results of figure 4 the force vector of figure 11 describes a curve which is not very far away from an ideal circular shape. An advantage of this design is the common direction of rotation of the Lorentz and the Maxwell force vectors (figures 12 and 13). In the superposition the two (non ideal) components complement each other to a curve with a relatively small amplitude variation. From the mechanical point of view the exterior rotor design can lead to better motor performance concerning torque ripple and cogging torque. Owing to the higher inertia the dynamic behavior of course is worse than in the interior rotor variant.

CONCLUSIONS

Owing to the integration of both the torque and the levitation force, windings in the stator bearingless permanent motors are distinguished by a very compact motor construction. In some applications like pumps, fans or blowers with no special demands on the starting torque a single-phase motor can be well suited for low cost devices.

The proposed motor design with only four concentrated coils leads to non-circular force locus curves. The shape of these curves is formed by Lorentz and Maxwell force components acting on the current layers and on the surface of the ferromagnetic materials. Finite element calculations show that the force characteristic is strongly influenced by the rotor design. The exterior rotor design shows better results than the interior rotor variant. An advantage of the exterior design is the common direction of rotation of the Lorentz and the Maxwell force vectors. In the superposition the two (non ideal) components complement each other to a curve with a small variation of the force amplitude.

ACKNOWLEDGMENT

The project was kindly supported by the Laboratory for Electrical Engineering Design (EEK) of Swiss Federal Institute of Technology, Zurich (ETH Zurich) and Sulzer Electronics AG, CH-Winterthur.

REFERENCES

[1] W. Amrhein, S. Silber, "Bearingless Single-Phase Motor with Concentrated Full Pitch Windings in Interior Rotor Design", Proc. ISMB-6, Cambridge, MA USA, pp. 486-496, August 1998.

[2] S. Silber, W. Amrhein, "Bearingless Single-Phase Motor with Concentrated Full Pitch Windings in Exterior Rotor Design," Proc. ISMB-6, Cambridge, MA USA, pp. 476-485, August 1998.

[3] R. Schöb, N. Barletta, "Principle and application of a bearingless slice motor", Proc. ISMB-5, Kanazawa, Japan, pp. 313-318, Aug. 1996.

[4] R. Schöb, Beiträge zur lagerlosen Asynchronmaschine, Dissertation, ETH Zürich, 1993

[5] J. Bichsel, Beiträge zum lagerlosen Elektromotor, Dissertation, ETH Zürich, 1990.

[6] R. Schöb, J. Bichsel, "Vector control of the bearingless motor", Proc. 4th Int. Symp. Magn. Bearings, Zurich, Switzerland, 1994

[7] H. Bleuler, H. Kawakatsu, W. Tang, W. Hsieh, D.K. Miu, Y. Tai, F. Moesner, M. Rohner, "Micromachined active magnetic bearings", Proc. ISMB-4, Zürich, Switzerland , pp. 349-352, August 1994.

[8] T. Ohishi, Y. Okada, K. Dejima, „Analysis and design of a concentrated wound stator for synchronous-type levitated motor", Proc. ISMB-4, Zürich, Switzerland, pp. 201-206, August 1994.

[9] M. Oshima, S. Miyazawa, T. Deido, A. Chiba, F. Nakamura, T. Fukao, "Characteristics of a Permanent Magnet Type Bearingless Motor", IEEE Trans. Ind. Applic., vol. 32/2, pp. 363-369, March/April 1996.

[10] Y. Okada, S. Miyamoto, T. Ohishi, "Levitation and Torque Control of Internal Permanent Magnet Type Bearingless Motor", IEEE Trans. on Control Syst. Techn., vol. 4/5, pp. 565-571, September 1996.
[11] M. Ooshima, A. Chiba, T. Fukao, M. A. Rahman, "Design and Analysis of Permanent Magnet-Type Bearingless Motors", IEEE Trans. on Indus. Electr., vol. IE-43, no. 2, pp. 292-299, April 1996.

FIGURES

Figure 1. Bearingless motor in a pump application (interior and exterior rotor design).

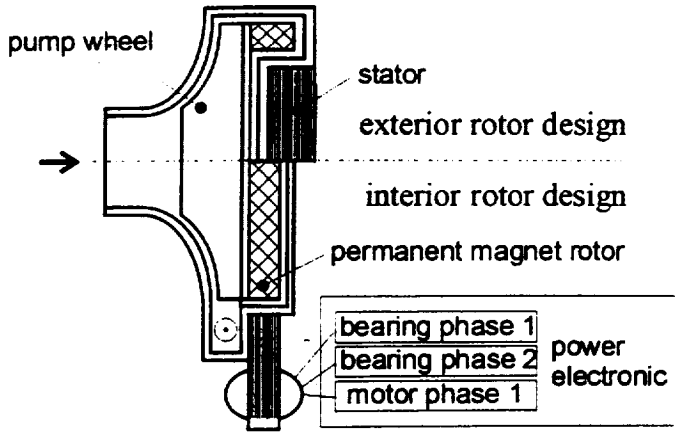

Figure 2. Principle construction of the bearingless motor in exterior rotor design.

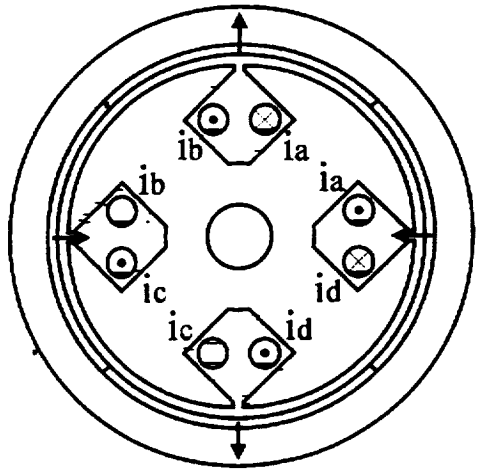

Figure 3. Simplified motor model in interior rotor design.

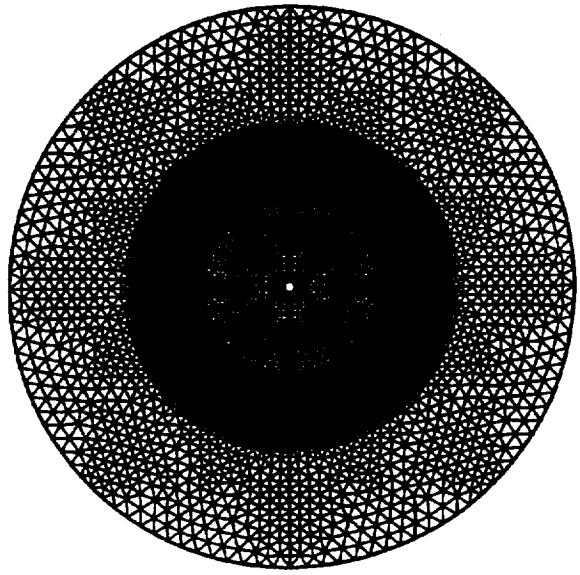

Figure 4. Force locus curve of the motor in interior rotor design (rectangular flux density distribution).

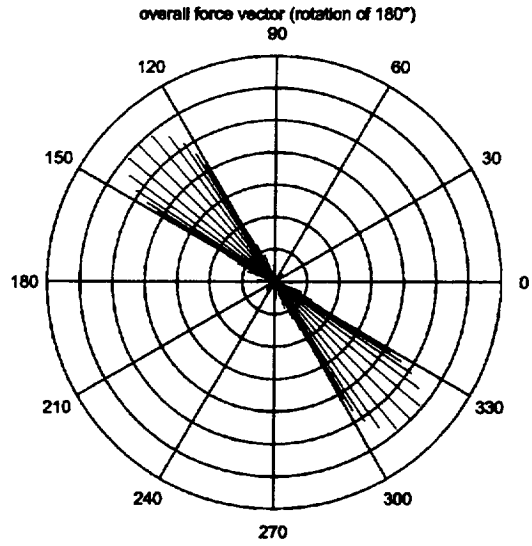

Figure 5. Field distribution for rotor position δ=0° .

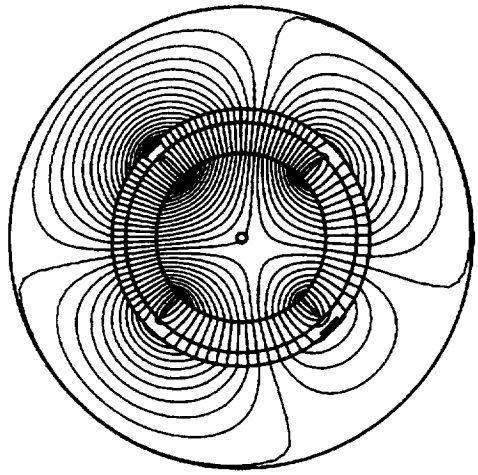

Figure 6. Field distribution for rotor position δ=90°.

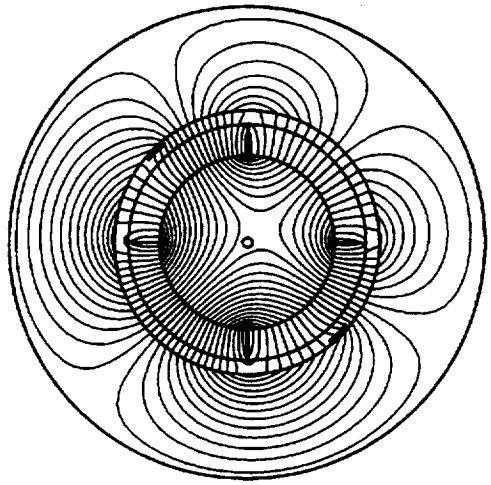

Figure 7. Lorentz forces of figure 4.

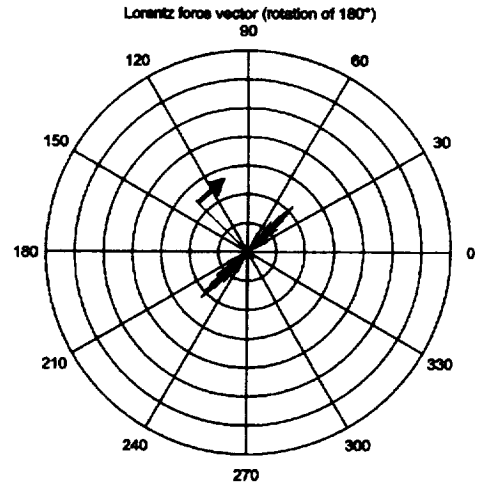

Figure 8. Maxwell forces of figure 4.

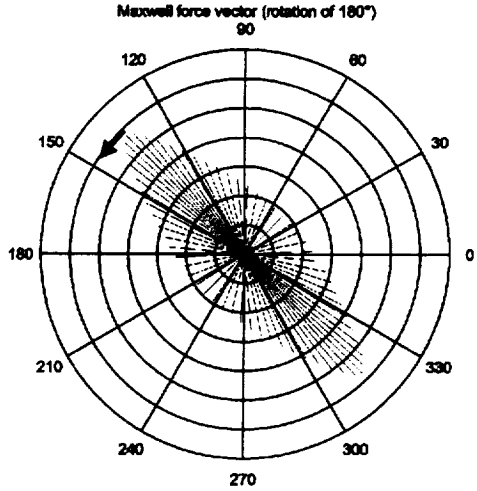

Figure 9. Force locus curve of the motor in interior rotor design (sinusoidal flux density distribution).

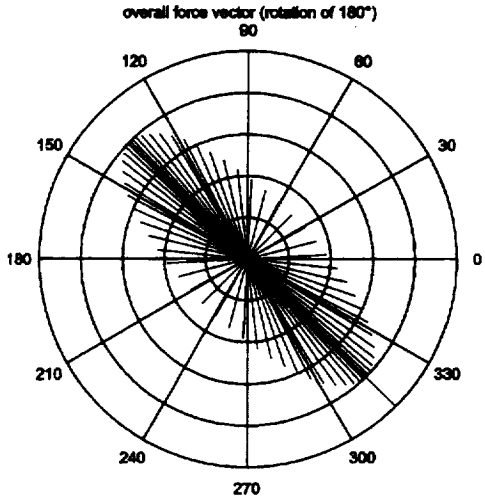

Figure 10. Simplified motor model in interior rotor design.

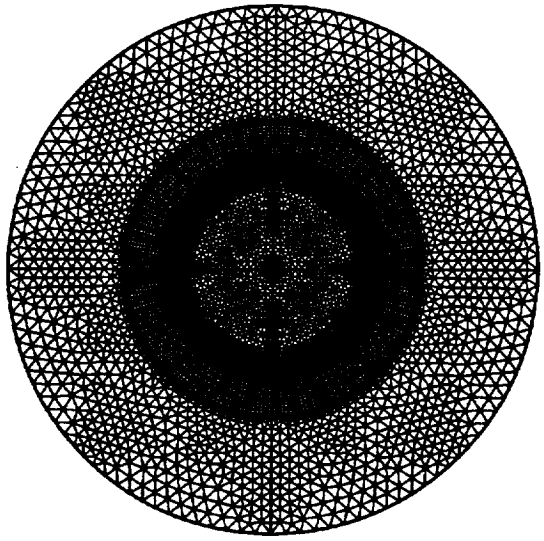

Figure 11. Force locus curve of the motor in exterior rotor design (rectangular flux density distribution).

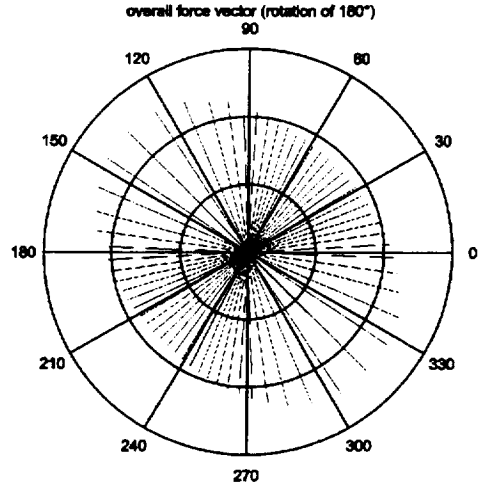

Figure 12. Lorentz forces of figure 11.

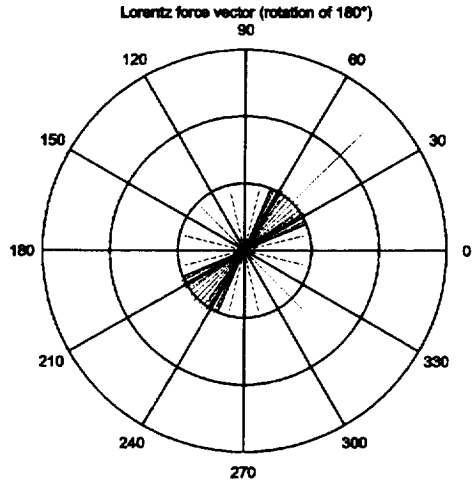

Figure 13. Maxwell forces of figure 11.